Report

Cell Reports

# Reversion of *FMR1* Methylation and Silencing by Editing the Triplet Repeats in Fragile X iPSC-Derived Neurons

## Graphical Abstract

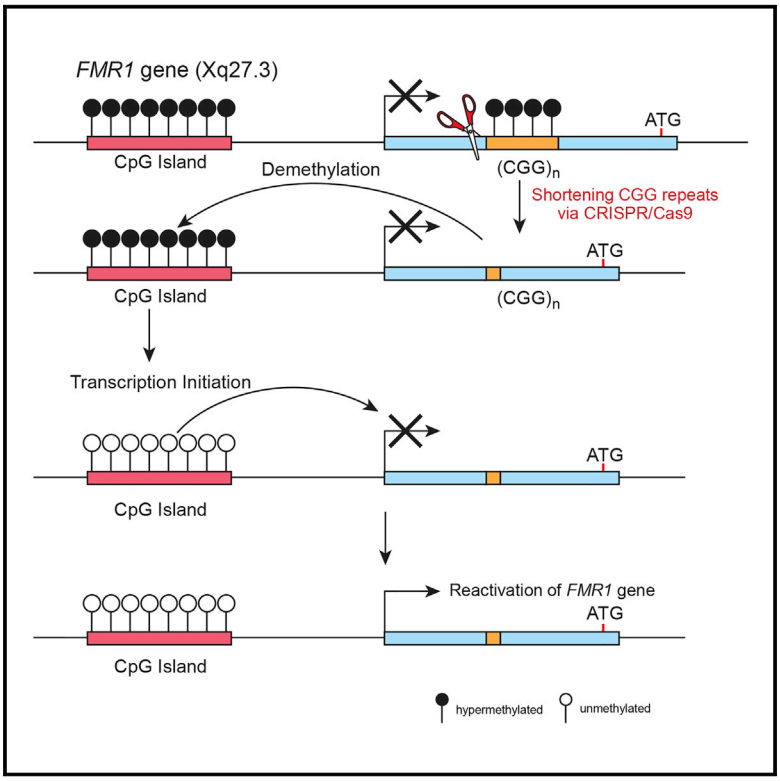


## Highlights

- Fragile X iPSCs were edited with CRISPR/Cas9 to remove the CGG repeats in the *FMR1* gene
- Edited FXS iPSCs showed complete ablation of the repeats and expression of *FMR1* mRNA
- The *FMR1* promoter in edited FXS iPSCs showed a near complete demethylation
- Edited FXS iPSCs that differentiated to mature neurons showed reactivation of FMRP

## Authors

Chul-Yong Park, Tomer Halevy, Dongjin R. Lee, ..., Ofra Yanuka, Nissim Benvenisty, Dong-Wook Kim

## Correspondence

nissimb@cc.huji.ac.il (N.B.), dwkim2@yuhs.ac (D.-W.K.)

## In Brief

Park et al. demonstrate deletion of the extended CGG repeats in fragile X-derived induced pluripotent stem cells. The ablation of the triple repeats caused demethylation of the *FMR1* promoter as well as reactivation of the gene both at the mRNA and protein levels that persisted through differentiation into mature neurons.

Park et al., 2015, Cell Reports *13*, 234–241
October 13, 2015 ©2015 The Authors
http://dx.doi.org/10.1016/j.celrep.2015.08.084

OPEN ACCESS
CellPress

Cell Reports
Report

# Reversion of *FMR1* Methylation and Silencing by Editing the Triplet Repeats in Fragile X iPSC-Derived Neurons

Chul-Yong Park,[1,3] Tomer Halevy,[2,3] Dongjin R. Lee,[1] Jin Jea Sung,[1] Jae Souk Lee,[1] Ofra Yanuka,[2] Nissim Benvenisty,[2,*] and Dong-Wook Kim[1,*]

[1]Department of Physiology and Brain Korea 21 Plus Project for Medical Science, Yonsei University College of Medicine, Seoul 120-752, Korea
[2]The Azrieli Center for Stem Cells and Genetic Research, Department of Genetics, Institute of Life Sciences, the Hebrew University, Givat-Ram, Jerusalem 91904, Israel
[3]Co-first author
*Correspondence: nissimb@cc.huji.ac.il (N.B.), dwkim2@yuhs.ac (D.-W.K.)
http://dx.doi.org/10.1016/j.celrep.2015.08.084


## SUMMARY

**Fragile X syndrome (FXS) is the most common form of inherited intellectual disability, resulting from a CGG repeat expansion in the fragile X mental retardation 1 (*FMR1*) gene. Here, we report a strategy for CGG repeat correction using CRISPR/Cas9 for targeted deletion in both embryonic stem cells and induced pluripotent stem cells derived from FXS patients. Following gene correction in FXS induced pluripotent stem cells, *FMR1* expression was restored and sustained in neural precursor cells and mature neurons. Strikingly, after removal of the CGG repeats, the upstream CpG island of the *FMR1* promoter showed extensive demethylation, an open chromatin state, and transcription initiation. These results suggest a silencing maintenance mechanism for the *FMR1* promoter that is dependent on the existence of the CGG repeat expansion. Our strategy for deletion of trinucleotide repeats provides further insights into the molecular mechanisms of FXS and future therapies of trinucleotide repeat disorders.**

## INTRODUCTION

Fragile X syndrome (FXS) is the most common inherited form of intellectual disability with an incidence in males of one in 3,600, and it is caused by the silencing of the fragile X mental retardation 1 (*FMR1*) gene located on chromosome X (Crawford et al., 2001; O'Donnell and Warren, 2002; Penagarikano et al., 2007). The causative mutation in FXS is a triple nucleotide CGG repeat expansion located in the 5′-UTR of *FMR1* (Fu et al., 1991; Verkerk et al., 1991). Although healthy individuals harbor between 5 and 55 copies of the CGG repeats, affected patients harbor more than 200 copies and are considered as having a full mutation (Pearson et al., 2005). It has been demonstrated that the silencing of *FMR1* in patients with a full mutation is correlated with abnormal DNA methylation and epigenetic changes in the CGG repeats (Coffee et al., 2002; Urbach et al., 2010; Eiges et al., 2007; Avitzour et al., 2014; Tabolacci et al., 2008).

We previously have generated models for FXS in embryonic stem cells (ESCs) (Eiges et al., 2007) and in induced pluripotent stem cells (iPSCs) (Urbach et al., 2010), and, using these models, we have demonstrated both the temporal silencing of *FMR1* during embryonic development and the ability to generate FXS neurons. We also have shown that the demethylating agent 5-azacytidine (5-AzaC) can induce reactivation of *FMR1* expression in FXS-iPSCs and partial demethylation of the *FMR1* promoter, suggesting a direct effect of methylation on the silencing of *FMR1* (Bar-Nur et al., 2012). However, the interrelationship between the CGG repeats found at the 5′-UTR of *FMR1* and the silencing of the gene is still obscure. It is also unclear whether a silenced methylated gene promoter could be demethylated upon removal of the downstream CGG repeats, and whether these changes would in turn affect gene expression.

The prokaryotic Type II clustered regularly interspaced short palindromic repeat (CRISPR)/CRISPR-associated 9 (Cas9) system, also known as RNA-guided endonucleases (RGENs), acts as an adaptive immune response in bacteria and archaea (Horvath and Barrangou, 2010; Wiedenheft et al., 2012). During the last few years, this system has been remodeled and adapted for genome editing (Cong et al., 2013; Mali et al., 2013; Cho et al., 2013; Wang et al., 2013). The Cas9 nuclease (derived from *Streptococcus pyogenes*) can be guided by a single-guide RNA (sgRNA) that is complementary to the target DNA via Watson-Crick base pairing and via the 5′-NGG motif known as the protospacer adjacent motif (PAM) (Jinek et al., 2012). The guided delivery of the Cas9 nuclease to its target site results in a DNA double-strand break (DSB) 3 bp upstream of the PAM sequence. The introduction of a DSB at a genomic locus increases the occurrence of insertion/deletion mutations or homology-directed recombination (HDR) by cellular repair mechanisms.

Patient-specific iPSCs derived from affected individuals are suggested as a promising therapeutic source to treat and study

genetic disorders by correcting the causal mutations. In this work, we utilized the RGEN system to edit the CGG repeats located at the 5′-UTR of *FMR1.* We show that removal of the CGG repeats can induce reactivation of silenced *FMR1* gene expression in FXS iPSC systems and their derivatives. Furthermore, we demonstrate complete DNA demethylation of the *FMR1* promoter in FXS-edited lines, suggesting that the DNA methylation status of the *FMR1* promoter in FXS iPSCs is dependent upon the CGG repeats and is constantly maintained according to the methylation status of the repeats. This study demonstrates that a full mutation of a CGG repeat expansion can be corrected using engineered nucleases in a patient-specific iPSC system without the use of template DNA for correction. This strategy may provide a promising applicable approach in the study of gene and cell therapy for future treatment of FXS and other genetic diseases caused by abnormal trinucleotide repeat expansions.

## RESULTS

### Sequence Analysis of the 5′-UTR within the *FMR1* Gene

To identify DNA sequences in the *FMR1* gene that would enable deletion of the CGG repeats, we determined the sequence of the CGG repeats and their flanking regions (herein termed upstream and downstream of the CGG repeats) in wild-type (WT) and FXS iPSCs and ESCs. We first amplified the 5′-UTR from WT cell lines using the primer sets FMR1-F and FMR1-R (Figure S1A). In the case of FXS iPSCs and ESCs, we amplified the upstream and downstream regions of the CGG repeats separately, using FMR1-F/FMR1-R1 or FMR1-F1/FMR1-R primers, respectively (Figure S1A). This is because conventional PCR methods have difficulty amplifying fully mutated CGG repeats that are more than 200 copies long, which is the case in FXS patients. Indeed, previous reports have indicated that the FXS iPSCs used in this study harbored more than 450 repeats, and the FXS ESCs in this study harbored more than 200 CGG repeats (Gray et al., 2007; Eiges et al., 2007). Our WT cells showed repeated structures of nine to ten CGG trinucleotides linked with or without a single AGG trinucleotide (Figure S1B; Table S1). Interestingly, we found that the sequences of the flanking upstream and downstream regions in WT and patient-derived cells were identical (Figure S1B). The *FMR1* gene resided on the X chromosome and appeared in only one allele in male cells; we thus hypothesized that DSB-induced deletions of the CGG repeats would be resolved by non-homologous end joining (NHEJ) between the sequences flanking the triplet repeats.

### RGEN-Induced Mutations within the *FMR1* Gene in HEK293T Cells

Next, we generated RGEN composed of the Cas9 nuclease and sgRNA that targeted the end of the upstream sequence of the CGG repeats (Figure 1A). To confirm the RGEN genome-editing activities, a T7 endonuclease I (T7E1) assay was performed in HEK293T cells. The RGEN activity was relatively high, inducing mutations with a frequency of 41% at the target site (Figure 1B). In additional sequencing analyses, large deleted sequences as well as small insertions and deletions (indels) were found at the RGEN target site (Figure S1C). Because off-target mutations may cause undesirable effects when using RGEN systems (Fu et al., 2013; Hsu et al., 2013; Pattanayak et al., 2013; Cho et al., 2014), we investigated whether these mutation types were induced by the RGEN system used in this study. The four potential off-target sites most similar to the on-target site in the human genome were searched using the Cas-OFFinder program (Figure S1D). We then verified that the RGEN system used in this study did not create any detectable off-target mutations at these sites using the T7E1 assay (Figure S1E).

### Targeted Genomic Editing of CGG Repeats in Patients' iPSCs and ESCs

To correct FXS in the patients' cells, we utilized our engineered RGENs to edit FXS iPSCs and FXS ESCs. Following electroporation of Cas9 and sgRNA plasmids into WT cells, FXS iPSCs, and FXS ESCs, PCR-based genotyping analysis was performed to screen for edited clones. Of all the edited WT iPSC and WT ESC clones analyzed, only clones with a CGG repeat deletion of approximately 90 bp from their parental lines were selected for further analysis as controls (Table S1). In FXS iPSCs and FXS ESCs, we only selected clones that had PCR products of similar size to those of the 90 bp-deleted WT cells (Figure 1C). Following the screen and further passaging, two to three edited clones from each cell type with CGG repeat deletions were established out of approximately 100 colonies (2%–3% efficiency) and confirmed using PCR-based genotyping (Figure 1C). All edited clones displayed a deletion of the CGG repeat sequence at the 5′-UTR of *FMR1* (Figure 1D). This result demonstrates that targeted DSBs upstream of the CGG repeat are induced by the Cas9 nuclease and can cause large deletions of abnormally mutated repeats. Finally, to verify a complete ablation of the CGG repeats in the selected edited FXS iPSCs, we analyzed our FXS iPSCs as well as the edited FXS iPSC clones E1 and E3 using the AmplideX *FMR1* PCR kit. Analysis revealed that, while the parent FXS iPSCs harbored more than 200 repeats, the edited FXS iPSC clones showed no detection of CGGs (Figure S1F).

### Reactivation of *FMR1* Gene Expression in Edited FXS iPSC and FXS NPC Clones

Based on the encouraging results of the genomic DNA editing, we analyzed whether deletion of the CGG repeats would lead to the reactivation of *FMR1*. To assess the reactivation of the silenced *FMR1* gene, mRNA levels were evaluated in WT and FXS iPSCs, in both edited and non-edited isogenic cell lines, using qPCR analysis. Unlike in FXS patient iPSC models, the expression of *FMR1* remains active in FXS ESCs, and silencing is sometimes obtained only after a very long differentiation into mature neurons (Urbach et al., 2010). Because of this difference between patient-derived iPSCs and ESCs, we chose to focus on reactivation of the *FMR1* gene by genome editing in the iPSC model system. Interestingly, we found that, in edited FXS iPSCs (FXS iPSC clones E1 and E3), the reactivation of the silenced *FMR1* mRNA occurred after deletion of the CGG repeats. We also found that *FMR1* mRNA levels were restored to levels similar to those seen in control WT cells. Furthermore, the deletion itself did not show any major change to the transcription of *FMR1* in edited WT iPSCs compared with their parental non-edited cells (Figure 1E).

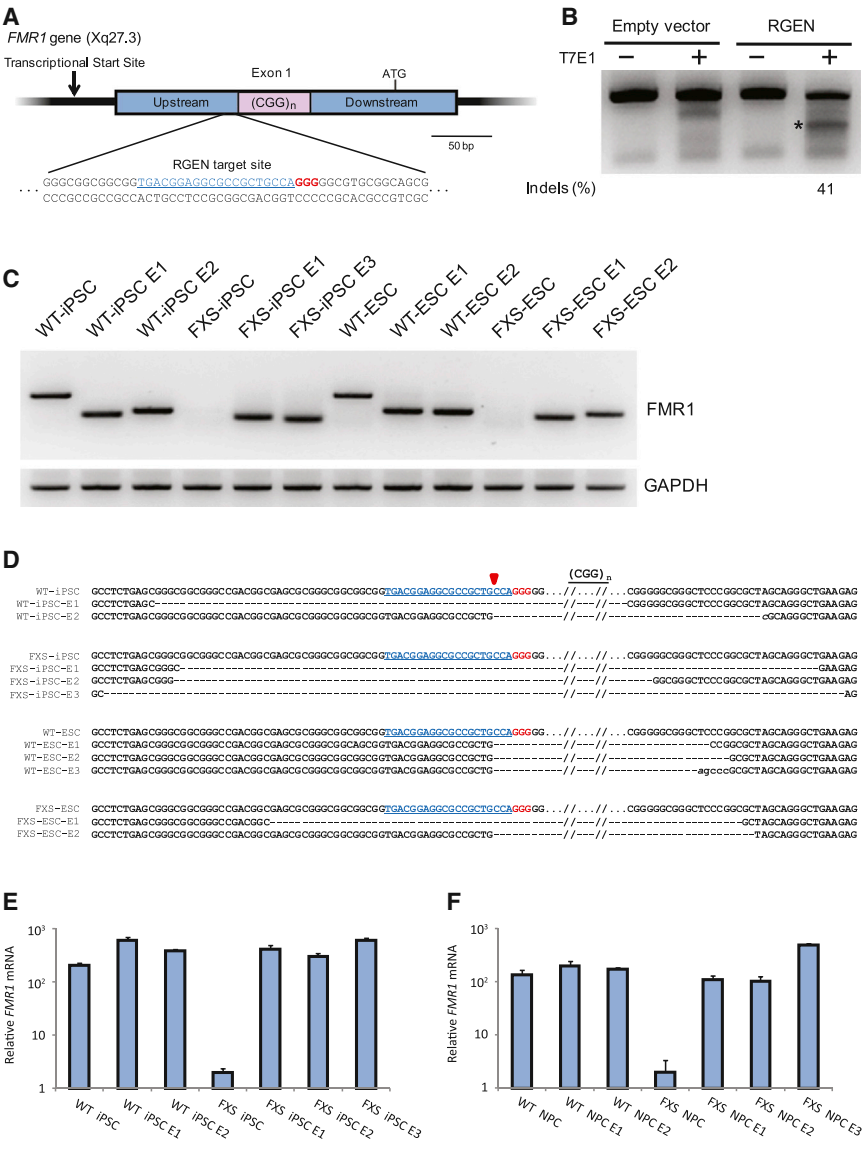


**Figure 1. RGEN-Induced Mutations and Reactivation of *FMR1***

(A) The RGEN-binding site is shown in a schematic view of the *FMR1* 5′-UTR; the PAM sequence is shown in red.

(B) Mutations at the RGEN target site were estimated in HEK293T cells by the T7E1 assay. The asterisk indicates the predicted position of DNA bands cleaved by T7E1.

(C) PCR analysis of genomic DNA from wild-type (WT), patient (FXS), and edited (E) lines is shown.

(D) PCR products amplified from each cell type were analyzed for their sequences. Each RGEN target sequence is underlined, respectively. The PAM sequence is indicated in red, the cleavage site is represented as the red triangle, the deleted bases are represented as dashes, and the inserted bases are represented as lowercase letters. The expression of *FMR1* mRNA in WT cells (WT), FXS patient cells (FXS), and edited clones (E1 to E3) was analyzed.

(E and F) The qPCR was used to detect expression of the *FMR1* gene in undifferentiated cells (E) and expendable NPCs (F). GAPDH expression was used for normalization. Error bars represent SE (n = 3 independent experiments).

We first analyzed the methylation status of the *FMR1* promoter in iPSCs in order to determine whether the deletion of the CGG repeats affected the upstream CpG island of the promoter. Using pyrosequencing, we analyzed 22 CpG sites between −395 to −256 bp from the *FMR1* transcription start site (Figure 2A). The results indicated that, prior to the removal of the CGG repeats in FXS iPSCs by RGEN, all CpG sites were hypermethylated, with most sites reaching 100% methylation (Figure 2B). When analyzing the same 22 CpG sites at the *FMR1* promoter in our edited FXS iPSC clones, we detected a dramatic demethylation of the promoter, with many CpG sites reaching methylation levels similar to those observed in WT cells (Figure 2B). Quantification of the pyrosequencing results showed that the average methylation level of the WT iPSC promoter was 0.4%, and in FXS iPSCs the average promoter methylation reached 87.4%. When analyzing the edited FXS iPSCs, we detected a striking decrease in average methylation of the promoter, which was only 10% in FXS iPSC clone E1 and a mere 0.8% in FXS iPSC clone E3, similar to WT iPSCs (Figure 2C).

Methylation levels of the *FMR1* promoter also were analyzed in NPCs derived from the aforementioned WT, FXS, edited WT, and edited FXS iPSCs. Similar to what was observed in the iPSCs, NPCs also showed a significant change in promoter methylation levels between edited and non-edited FXS clones. Although both WT NPCs and edited WT NPCs showed hypomethylation, with almost all sites being completely non-methylated,

To ensure that the reactivation seen in iPSCs is retained through neural differentiation, we induced neural rosettes from WT, FXS-edited, and non-edited isogenic cell lines. No difference in the formation rate of neural rosettes was observed between edited iPSC and ESC lines when compared with their parental lines, indicating that all lines used in the study have a similar potential to differentiate into early neural cells (Figure S2A). Transcription of *FMR1* was maintained in neuronal precursor cells (NPCs) differentiated from all edited FXS iPSC lines (namely, FXS iPSC E1, E2, and E3), with similar expression levels to those seen in WT iPSCs (Figure 1F).

## Analysis of the Methylation Status within the Promoter Region of *FMR1*

After successfully reactivating *FMR1* at the RNA level, we sought to understand whether the changes seen in expression correlated with epigenetic changes in the promoter region of *FMR1*.

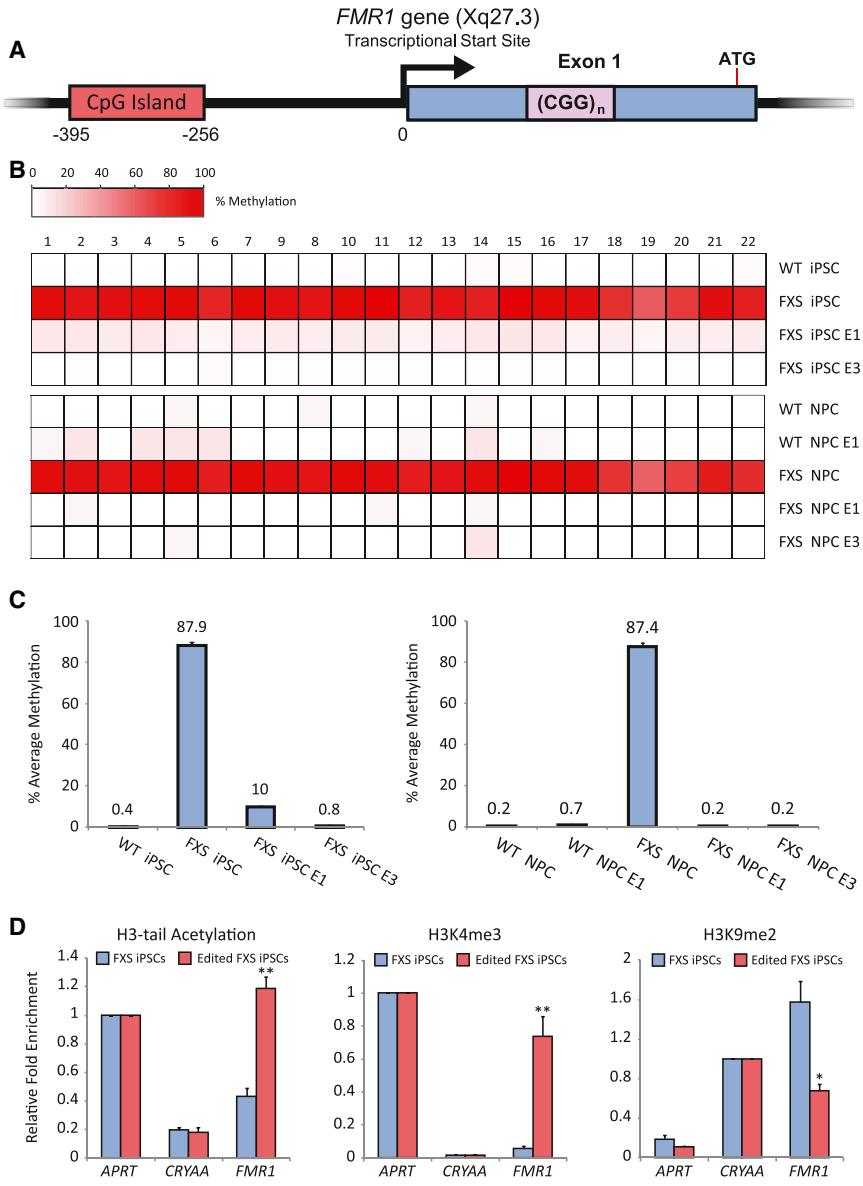


**Figure 2. Methylation and Chromatin Conformation Analysis of the *FMR1* Promoter**

(A) The 22 CpG sites used for the methylation analysis are clustered at the promoter of *FMR1*, −395 to −256 bp from the gene's transcription start site.

(B) Pyrosequencing was performed on 22 CpGs of the *FMR1* promoter for WT, FXS, and edited FXS iPSCs (top), as well as on both edited and non-edited WT and FXS NPCs (bottom). FXS iPSCs show full methylation prior to gene editing and extensive de-methylation after editing for most sites (top). In NPCs, both WT and edited WT NPCs show hypomethylation, and FXS NPCs show hypermethylation of the promoter in all analyzed sites. In contrast to FXS NPCs, both edited FXS NPC clones show strong hypomethylation, with most sites showing methylation levels similar to WT levels (bottom).

(C) Quantification of methylation levels at all CpG sites shows the average percentage of methylation for each cell type. WT iPSCs show hypomethylation and FXS iPSCs show hypermethylation. After editing the CGG repeats, FXS iPSCs show hypomethylation, similar to WT iPSCs (left graph). Similar percentages of methylation were observed in NPCs derived from the aforementioned cells (right graph).

(D) Chromatin immunoprecipitation was performed on FXS iPSCs and edited FXS iPSCs. Graphs show relative fold enrichment for different chromatin markers. *APRT* marks open chromatin, *CRYAA* marks closed chromatin, and *FMR1* was compared with both. Results show that the *FMR1* promoter in FXS iPSCs resembles markers of closed chromatin, and, after editing, the promoter is enriched for markers of open chromatin. Error bars represent SE; *$p < 0.05$, **$p < 0.005$, using Student's t test.

FXS NPCs displayed hypermethylation with most sites reaching close to 100% methylation (Figure 2B). In the edited clones, both FXS NPC clones showed clear hypomethylation, with most sites completely unmethylated (Figure 2B). Quantification of all sites showed that the average methylation of the *FMR1* promoter in WT and edited WT NPCs was 0.2% and 0.7%, respectively (Figure 2C). In FXS NPCs, average promoter methylation was as high as 87.4%; the average promoter methylation of edited FXS NPCs reached only 0.2% in both clones, similar to the levels observed in WT NPCs (Figure 2C).

To analyze changes to the chromatin structure of the *FMR1* gene, we employed chromatin immunoprecipitation against histone 3 tail acetylation (H3 Ace) and histone 3 K4 methylation (H3 K4meth), which indicate a transcriptionally active chromatin state, and against histone 3 K9 methylation (H3 K9meth), which indicates a repressed chromatin state and is associated with *FMR1* silencing (Coffee et al., 1999, 2002). Both markers for active chromatin, H3 Ace and H3 K4meth, were markedly upregulated following the CGG repeat editing, and the repressive chromatin marker H3 K9meth was significantly downregulated (Figure 2D). In addition, expression levels of *APRT*, *CRYAA*, and *FMR1* were analyzed in WT and FXS iPSCs using RT-PCR. Expression analysis verified the correlation between expression and epigenetic modifications (Figure S2B). These results indicate that the ablation of the CGG repeats had an epigenetic effect on the methylation status and chromatin state of the *FMR1* promoter.

## Restoration of FMRP Levels in Edited FXS Clones

Lastly, we validated the presence of the FMR1 protein (FMRP), using immunocytochemistry staining in edited iPSC lines as well as their parental lines. As expected, undifferentiated FXS iPSCs stained negative for FMRP, in contrast to WT iPSCs, which stained positive for FMRP (Figure 3A). This result was further validated by western blotting to ensure a more sensitive

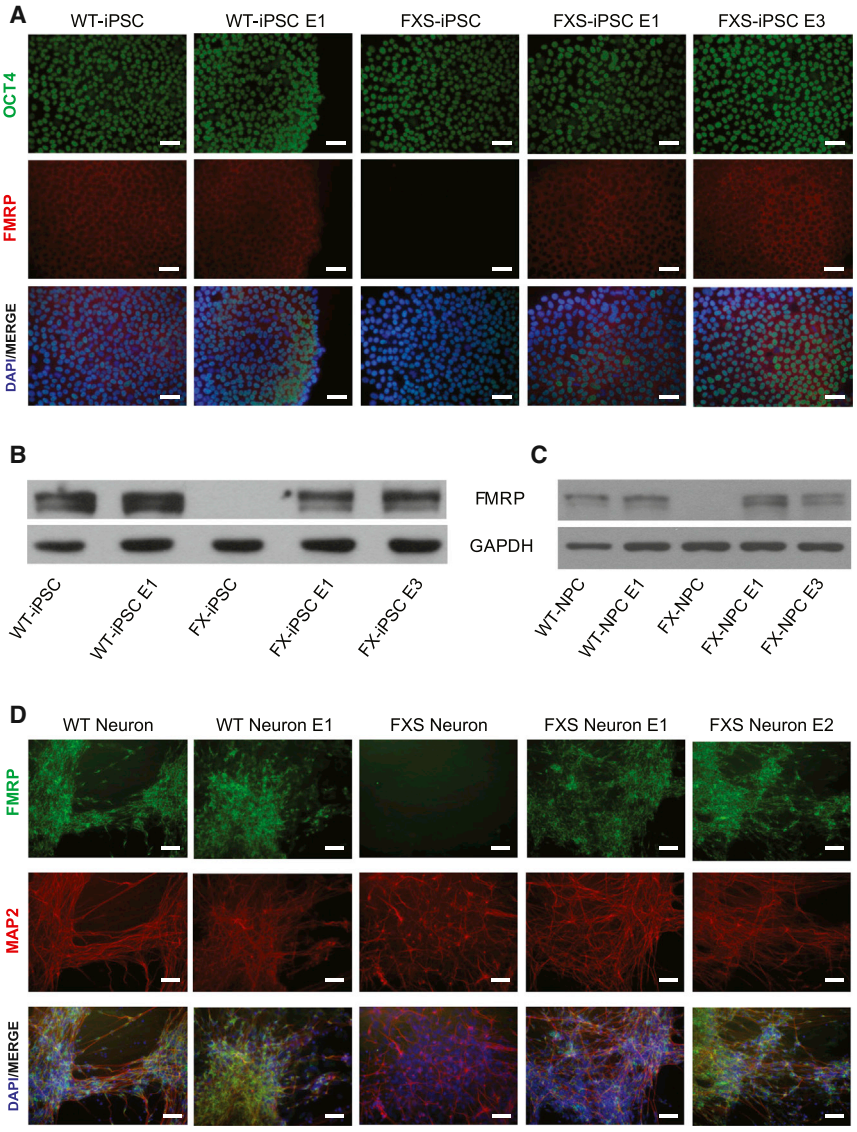


**Figure 3. Restoration of FMRP in Edited FXS Cells**

(A) Detection of FMRP in WT iPSCs (WT), patients' iPSCs (FXS), and edited clones (E1 and E3) by immunochemistry. Undifferentiated cells grown on feeder-free media were fixed and stained with the indicated antibodies. DAPI signals (blue) indicate the total cell presence in the image. Scale bars, 50 μm.

(B) Immunoblot analysis of FMRP in WT, edited WT (E1), FXS, and edited FXS clones (E1 and E3). GAPDH was used as a loading control.

(C) The detection of FMRP in NPCs of each cell type was confirmed by immunoblot analysis. GAPDH was used as a loading control.

(D) The detection of FMRP in WT, patient (FXS), and edited iPSC clones (E1 and E2) by immunochemistry. Mature neurons differentiated for 60 days from each line were fixed and stained with the indicated antibodies. DAPI signals (blue) indicate the total cell presence in the image. Scale bars, 50 μm.

detection of FMRP (Figure 3B). In line with our transcription and epigenetic results, we found that the levels of FMRP were restored in the edited FXS iPSC lines E1 and E3. All edited lines showed similar staining of OCT4 compared with their parental lines (Figure 3A). Furthermore, other pluripotency markers showed similar expression levels in both edited lines and their parental lines, as detected by qPCR analysis (Figure S2C). This result suggests that the procedure leading to the deletion of the repeats did not have a negative effect on the undifferentiated status of the edited clones. Edited ESC lines also were analyzed and showed staining of FMRP similar to that of their isogenic parental ESCs (Figure S2D). Next, NPCs derived from FXS iPSC clones E1 and E3 also were analyzed for the presence of FMRP by western blotting, in which they showed high levels of FMRP (Figure 3C).

We further examined whether the presence of FMRP could be sustained in mature neurons derived from edited FXS iPSC clones. To address this issue, WT and FXS iPSCs as well as their isogenic edited lines were differentiated into mature neurons (Kim et al., 2010, 2012). We then stained these preparations for FMRP and microtubule-associated protein 2 (MAP2), a mature neuron marker. All differentiated cell lines showed positive staining for MAP2, indicating successful differentiation into mature neurons (Figure 3D). Reassuringly, mature neurons differentiated from FXS iPSC clones E1 and E2 stained positive for FMRP, unlike neurons derived from their parental non-edited FXS iPSCs (Figure 3D). To investigate any potential effect of the reactivated protein, we analyzed gene expression of edited FXS mature neurons compared with their isogenic parentally derived neurons. Our gene expression analysis demonstrated that, of the few genes that were differentially expressed between edited and non-edited FXS neurons, there was enrichment for different glutamate receptor genes. Several glutamate receptor genes showed more than a 2-fold reduction in RNA levels after editing (Figure S2E), whereas other key neuronal genes displayed similar expression levels (Figure S2F). This result correlates with a previous study that found dysregulation of glutamate receptor activity in FXS neurons (Dölen et al., 2007). All together, the results show that genotypic correction generated by deletion of the abnormal repeats can restore *FMR1* gene expression and the levels of FMRP in FXS iPSCs and their neural derivatives.

## DISCUSSION

Trinucleotide repeat expansions play a role in several neurological, neurodegenerative, and neuromuscular disorders such as

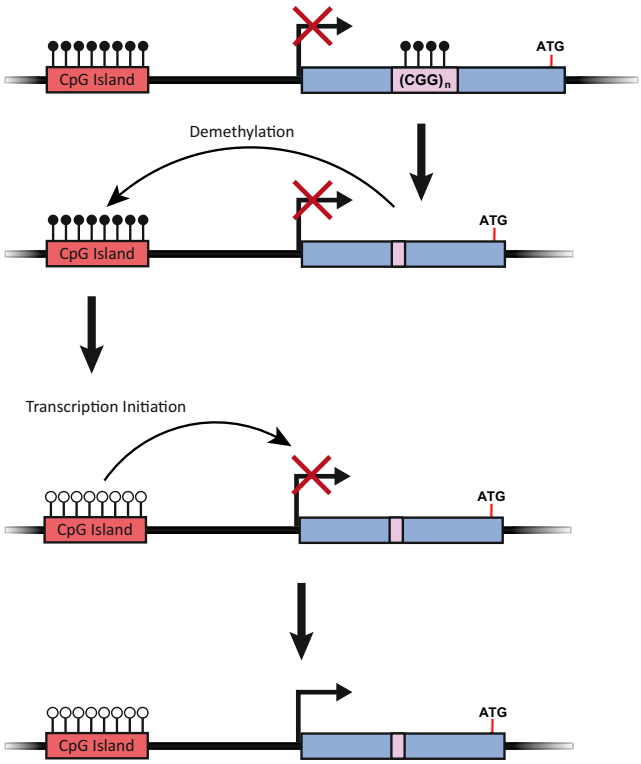


**Figure 4. *FMR1* Reactivation Model**

In FXS iPSCs, *FMR1* is silenced because of the presence of the full mutation of CGG repeats and their methylation, which affects the gene's promoter. After removal of the CGG repeats by RGEN, the promoter is released from its repressive markers and is completely demethylated. Demethylation of the *FMR1* promoter allows the gene to be transcribed and, hence, *FMR1* is reactivated.

Huntington's disease, FXS, spinocerebellar ataxia, and myotonic dystrophy (Pearson et al., 2005). In FXS, CGG repeat expansion in the 5′-UTR of the causative gene *FMR1* is linked to the development of the disease phenotype, although the disease mechanisms are not yet fully understood. During the last several years, correction of genetic defects using programmed nucleases has been attempted for several genetic diseases (Yusa et al., 2011; Sebastiano et al., 2011; Yin et al., 2014; Long et al., 2014; Maetzel et al., 2014; Li et al., 2015). Among these attempts, it has been demonstrated that expanded CAG repeats can be edited in Huntington's disease patient cells using the traditional homologous recombination (HR) or Cas9-mediated HR methods (An et al., 2012, 2014). However, in our study, we attempted a deletion-mediated correction of abnormal CGG repeat expansion without the use of a WT allele or the use of an exogenous donor sequence, but rather through NHEJ induced by the Cas9 nuclease.

Because individuals with less than 55 CGG trinucleotide repeats have normal *FMR1* expression and because a lower number of repeats allows for accurate sequencing of repeat portions and their flanking regions, we first tested our deletion-mediated correction approach in WT iPSCs and WT ESCs. As a result, CGG repeats, including some of the flanking regions, were successfully deleted in the WT cells. We then applied this approach to FXS patients' iPSCs and ESCs and succeeded in restoring *FMR1* expression. No difference was observed in the ability of edited cell lines to differentiate into NPCs and mature neurons when compared to the abilities of their parental cell lines.

In our sequencing analysis, we frequently observed deletions in corrected iPSC/ESC lines as well as in RGEN-transfected HEK293T cells. We speculate that some of these deletions may have been induced by microhomology-mediated end joining (MMEJ) that can cause variable-size deletions by base pairing between two short microhomologous sequences near the DSB region created by the engineered nucleases (McVey and Lee, 2008; Bae et al., 2014b). Our hypothesis that some deletions may have been caused by MMEJ is supported by the fact that numerous GC repeats were found in the upstream and downstream regions of CGG repeats, and by the fact that microhomologous sequences such as GGC and CGG were observed on both sides of the deletion in the case of 49- and 112-bp deletions (Figure S1C). Other deletions and insertions in general may have been induced by NHEJ.

The results of this study showed the reactivation of *FMR1* at the RNA, methylation, chromatin modification, and protein levels. Taking our current findings together with our previous results (Urbach et al., 2010; Eiges et al., 2007; Bar-Nur et al., 2012), we propose a model in which the presence of more than 200 CGG repeats is necessary, but not sufficient, for the silencing of *FMR1*. The presence of the full mutation is recognized during differentiation as a site for DNA methyltransferase activity, leading to full methylation of the CGG repeats. These epigenetic changes spread to the upstream and cause both DNA methylation of the CpG island at the *FMR1* promoter and the closed chromatin conformation in this region. In this work, we clearly demonstrate that removal of the CGG repeats in undifferentiated cells can lead to demethylation of the promoter, open chromatin conformation, and re-expression of the gene, all of which are sustained through neural rosette formation and long-term differentiation into mature neurons. These findings suggest a maintenance mechanism in which the methylation status of the promoter is constantly regulated according to the state of the repeats. Thus, when the repeats are removed, the *FMR1* promoter loses its methylation and shows an upregulation of active chromatin markers, thereby activating the *FMR1* gene (Figures 2D and 4).

The data presented demonstrate the ablation of full-mutation trinucleotide repeats and the complete reactivation of a gene using Cas9 nuclease without the use of a donor sequence for HR. Our Cas9-mediated method to correct trinucleotide repeats may be applied on patient-specific cells for gene correction of various short nucleotide repeat expansion-derived diseases, such as spinocerebellar ataxia and myotonic dystrophy. Further work on edited FXS iPSCs should be done to understand the full impact of the reactivation of FMRP and may reveal yet unknown functions of this important protein. This method for gene correction can be applied easily in many labs and holds a great potential for the study of trinucleotide repeat disorders as well as future research for novel therapies.

## EXPERIMENTAL PROCEDURES

### Cas9-Encoding Plasmid and Transfections

Cas9 and sgRNA expression plasmids were purchased from ToolGen. Potential off-target sites were computationally searched using Cas-OFFinder (http://www.rgenome.net/; Bae et al., 2014a). Human iPSCs and ESCs were pulsed with Cas9 and sgRNA-encoding plasmids as previously described (Park et al., 2014).

### Isolation of Clonal Cells and PCR Analysis

To isolate clonal populations of edited cells, each colony that had been identified by PCR with a deletion in the CGG repeats was dissociated into single cells and re-seeded onto a new feeder layer as previously described (Park et al., 2014).

### DNA Methylation Analysis

For DNA methylation analysis, genomic DNA was purified using the NucleoSpin Tissue kit (Macherey-Nagel) according to the manufacturer's protocol. Pyrosequencing was performed by EpigenDx according to standard procedures, with a unique set of primers developed by EpigenDx for targeting 22 CpG sites at the *FMR1* promoter.

### Chromatin Immunoprecipitation

For chromatin immunoprecipitation, FXS and edited FXS iPSCs were harvested, fixated, and cross-linked with formaldehyde solution, lysed, and sonicated. Chromatin was cleared using salmon sperm agarose beads (Millipore) for 1 hr at 4°C. Immunoprecipitation of chromatin was performed overnight using an anti-acetylated histone H3 antibody (Millipore 06599), an anti-methylated histone H3 at lysine 4 antibody (Millipore 17614), and an anti-methylated histone H3 at lysine 9 antibody (Millipore 17648). For more detailed information, see the Supplemental Experimental Procedures.

## SUPPLEMENTAL INFORMATION

Supplemental Information includes Supplemental Experimental Procedures, two figures, and two tables and can be found with this article online at http://dx.doi.org/10.1016/j.celrep.2015.08.084.

## AUTHOR CONTRIBUTIONS

C.-Y.P. and T.H. designed the research and prepared the manuscript. C.-Y.P., T.H., D.R.L., J.J.S., J.S.L., and O.Y. performed the experiments and interpreted the results. N.B. and D.-W.K. supervised the work and prepared the manuscript.

## ACKNOWLEDGMENTS

We thank Uri Weissbein from N.B.'s lab and Dong-Su Jang from the Medical Research Support Section, Yonsei University College of Medicine for graphical assistance. D.-W.K. was supported by grants from the National Research Foundation of Korea (the Bio & Medical Technology Development Program, 2012M3A9B4028631 and 2012M3A9C7050126) and from the Korean Ministry of Health & Welfare (A120254). N.B. is the Herbert Cohn Chair in Cancer Research. N.B. was partially supported by the Israel Science Foundation-Morasha Foundation (grant 1252/12), by the Rosetrees Trust, and by the Azrieli Foundation.

Received: June 2, 2015
Revised: July 30, 2015
Accepted: August 31, 2015
Published: October 1, 2015

## REFERENCES

An, M.C., Zhang, N., Scott, G., Montoro, D., Wittkop, T., Mooney, S., Melov, S., and Ellerby, L.M. (2012). Genetic correction of Huntington's disease phenotypes in induced pluripotent stem cells. Cell Stem Cell *11*, 253–263.

An, M.C., O'Brien, R.N., Zhang, N., Patra, B.N., De La Cruz, M., Ray, A., and Ellerby, L.M. (2014). Polyglutamine disease modeling: epitope based screen for homologous recombination using CRISPR/Cas9 system. PLoS Curr. *6*.

Avitzour, M., Mor-Shaked, H., Yanovsky-Dagan, S., Aharoni, S., Altarescu, G., Renbaum, P., Eldar-Geva, T., Schonberger, O., Levy-Lahad, E., Epsztejn-Litman, S., and Eiges, R. (2014). FMR1 epigenetic silencing commonly occurs in undifferentiated fragile X-affected embryonic stem cells. Stem Cell Reports *3*, 699–706.

Bae, S., Park, J., and Kim, J.S. (2014a). Cas-OFFinder: a fast and versatile algorithm that searches for potential off-target sites of Cas9 RNA-guided endonucleases. Bioinformatics *30*, 1473–1475.

Bae, S., Kweon, J., Kim, H.S., and Kim, J.S. (2014b). Microhomology-based choice of Cas9 nuclease target sites. Nat. Methods *11*, 705–706.

Bar-Nur, O., Caspi, I., and Benvenisty, N. (2012). Molecular analysis of FMR1 reactivation in fragile-X induced pluripotent stem cells and their neuronal derivatives. J. Mol. Cell Biol. *4*, 180–183.

Cho, S.W., Kim, S., Kim, J.M., and Kim, J.S. (2013). Targeted genome engineering in human cells with the Cas9 RNA-guided endonuclease. Nat. Biotechnol. *31*, 230–232.

Cho, S.W., Kim, S., Kim, Y., Kweon, J., Kim, H.S., Bae, S., and Kim, J.S. (2014). Analysis of off-target effects of CRISPR/Cas-derived RNA-guided endonucleases and nickases. Genome Res. *24*, 132–141.

Coffee, B., Zhang, F., Warren, S.T., and Reines, D. (1999). Acetylated histones are associated with FMR1 in normal but not fragile X-syndrome cells. Nat. Genet. *22*, 98–101.

Coffee, B., Zhang, F., Ceman, S., Warren, S.T., and Reines, D. (2002). Histone modifications depict an aberrantly heterochromatinized FMR1 gene in fragile x syndrome. Am. J. Hum. Genet. *71*, 923–932.

Cong, L., Ran, F.A., Cox, D., Lin, S., Barretto, R., Habib, N., Hsu, P.D., Wu, X., Jiang, W., Marraffini, L.A., and Zhang, F. (2013). Multiplex genome engineering using CRISPR/Cas systems. Science *339*, 819–823.

Crawford, D.C., Acuña, J.M., and Sherman, S.L. (2001). FMR1 and the fragile X syndrome: human genome epidemiology review. Genet. Med. *3*, 359–371.

Dölen, G., Osterweil, E., Rao, B.S., Smith, G.B., Auerbach, B.D., Chattarji, S., and Bear, M.F. (2007). Correction of fragile X syndrome in mice. Neuron *56*, 955–962.

Eiges, R., Urbach, A., Malcov, M., Frumkin, T., Schwartz, T., Amit, A., Yaron, Y., Eden, A., Yanuka, O., Benvenisty, N., and Ben-Yosef, D. (2007). Developmental study of fragile X syndrome using human embryonic stem cells derived from preimplantation genetically diagnosed embryos. Cell Stem Cell *1*, 568–577.

Fu, Y.H., Kuhl, D.P., Pizzuti, A., Pieretti, M., Sutcliffe, J.S., Richards, S., Verkerk, A.J., Holden, J.J., Fenwick, R.G., Jr., Warren, S.T., et al. (1991). Variation of the CGG repeat at the fragile X site results in genetic instability: resolution of the Sherman paradox. Cell *67*, 1047–1058.

Fu, Y., Foden, J.A., Khayter, C., Maeder, M.L., Reyon, D., Joung, J.K., and Sander, J.D. (2013). High-frequency off-target mutagenesis induced by CRISPR-Cas nucleases in human cells. Nat. Biotechnol. *31*, 822–826.

Gray, S.J., Gerhardt, J., Doerfler, W., Small, L.E., and Fanning, E. (2007). An origin of DNA replication in the promoter region of the human fragile X mental retardation (FMR1) gene. Mol. Cell. Biol. *27*, 426–437.

Horvath, P., and Barrangou, R. (2010). CRISPR/Cas, the immune system of bacteria and archaea. Science *327*, 167–170.

Hsu, P.D., Scott, D.A., Weinstein, J.A., Ran, F.A., Konermann, S., Agarwala, V., Li, Y., Fine, E.J., Wu, X., Shalem, O., et al. (2013). DNA targeting specificity of RNA-guided Cas9 nucleases. Nat. Biotechnol. *31*, 827–832.

Jinek, M., Chylinski, K., Fonfara, I., Hauer, M., Doudna, J.A., and Charpentier, E. (2012). A programmable dual-RNA-guided DNA endonuclease in adaptive bacterial immunity. Science *337*, 816–821.

Kim, D.S., Lee, J.S., Leem, J.W., Huh, Y.J., Kim, J.Y., Kim, H.S., Park, I.H., Daley, G.Q., Hwang, D.Y., and Kim, D.W. (2010). Robust enhancement of neural differentiation from human ES and iPS cells regardless of their innate difference in differentiation propensity. Stem Cell Rev. *6*, 270–281.

Kim, D.S., Lee, D.R., Kim, H.S., Yoo, J.E., Jung, S.J., Lim, B.Y., Jang, J., Kang, H.C., You, S., Hwang, D.Y., et al. (2012). Highly pure and expandable PSA-NCAM-positive neural precursors from human ESC and iPSC-derived neural rosettes. PLoS ONE *7*, e39715.

Li, H.L., Fujimoto, N., Sasakawa, N., Shirai, S., Ohkame, T., Sakuma, T., Tanaka, M., Amano, N., Watanabe, A., Sakurai, H., et al. (2015). Precise correction of the dystrophin gene in duchenne muscular dystrophy patient induced pluripotent stem cells by TALEN and CRISPR-Cas9. Stem Cell Reports *4*, 143–154.

Long, C., McAnally, J.R., Shelton, J.M., Mireault, A.A., Bassel-Duby, R., and Olson, E.N. (2014). Prevention of muscular dystrophy in mice by CRISPR/Cas9-mediated editing of germline DNA. Science *345*, 1184–1188.

Maetzel, D., Sarkar, S., Wang, H., Abi-Mosleh, L., Xu, P., Cheng, A.W., Gao, Q., Mitalipova, M., and Jaenisch, R. (2014). Genetic and chemical correction of cholesterol accumulation and impaired autophagy in hepatic and neural cells derived from Niemann-Pick Type C patient-specific iPS cells. Stem Cell Reports *2*, 866–880.

Mali, P., Yang, L., Esvelt, K.M., Aach, J., Guell, M., DiCarlo, J.E., Norville, J.E., and Church, G.M. (2013). RNA-guided human genome engineering via Cas9. Science *339*, 823–826.

McVey, M., and Lee, S.E. (2008). MMEJ repair of double-strand breaks (director's cut): deleted sequences and alternative endings. Trends Genet. *24*, 529–538.

O'Donnell, W.T., and Warren, S.T. (2002). A decade of molecular studies of fragile X syndrome. Annu. Rev. Neurosci. *25*, 315–338.

Park, C.Y., Kim, J., Kweon, J., Son, J.S., Lee, J.S., Yoo, J.E., Cho, S.R., Kim, J.H., Kim, J.S., and Kim, D.W. (2014). Targeted inversion and reversion of the blood coagulation factor 8 gene in human iPS cells using TALENs. Proc. Natl. Acad. Sci. USA *111*, 9253–9258.

Pattanayak, V., Lin, S., Guilinger, J.P., Ma, E., Doudna, J.A., and Liu, D.R. (2013). High-throughput profiling of off-target DNA cleavage reveals RNA-programmed Cas9 nuclease specificity. Nat. Biotechnol. *31*, 839–843.

Pearson, C.E., Nichol Edamura, K., and Cleary, J.D. (2005). Repeat instability: mechanisms of dynamic mutations. Nat. Rev. Genet. *6*, 729–742.

Penagarikano, O., Mulle, J.G., and Warren, S.T. (2007). The pathophysiology of fragile x syndrome. Annu. Rev. Genomics Hum. Genet. *8*, 109–129.

Sebastiano, V., Maeder, M.L., Angstman, J.F., Haddad, B., Khayter, C., Yeo, D.T., Goodwin, M.J., Hawkins, J.S., Ramirez, C.L., Batista, L.F., et al. (2011). In situ genetic correction of the sickle cell anemia mutation in human induced pluripotent stem cells using engineered zinc finger nucleases. Stem Cells *29*, 1717–1726.

Tabolacci, E., Moscato, U., Zalfa, F., Bagni, C., Chiurazzi, P., and Neri, G. (2008). Epigenetic analysis reveals a euchromatic configuration in the FMR1 unmethylated full mutations. Eur. J. Hum. Genet. *16*, 1487–1498.

Urbach, A., Bar-Nur, O., Daley, G.Q., and Benvenisty, N. (2010). Differential modeling of fragile X syndrome by human embryonic stem cells and induced pluripotent stem cells. Cell Stem Cell *6*, 407–411.

Verkerk, A.J., Pieretti, M., Sutcliffe, J.S., Fu, Y.H., Kuhl, D.P., Pizzuti, A., Reiner, O., Richards, S., Victoria, M.F., Zhang, F.P., et al. (1991). Identification of a gene (FMR-1) containing a CGG repeat coincident with a breakpoint cluster region exhibiting length variation in fragile X syndrome. Cell *65*, 905–914.

Wang, H., Yang, H., Shivalila, C.S., Dawlaty, M.M., Cheng, A.W., Zhang, F., and Jaenisch, R. (2013). One-step generation of mice carrying mutations in multiple genes by CRISPR/Cas-mediated genome engineering. Cell *153*, 910–918.

Wiedenheft, B., Sternberg, S.H., and Doudna, J.A. (2012). RNA-guided genetic silencing systems in bacteria and archaea. Nature *482*, 331–338.

Yin, H., Xue, W., Chen, S., Bogorad, R.L., Benedetti, E., Grompe, M., Kotelianksy, V., Sharp, P.A., Jacks, T., and Anderson, D.G. (2014). Genome editing with Cas9 in adult mice corrects a disease mutation and phenotype. Nat. Biotechnol. *32*, 551–553.

Yusa, K., Rashid, S.T., Strick-Marchand, H., Varela, I., Liu, P.Q., Paschon, D.E., Miranda, E., Ordóñez, A., Hannan, N.R., Rouhani, F.J., et al. (2011). Targeted gene correction of $\alpha$1-antitrypsin deficiency in induced pluripotent stem cells. Nature *478*, 391–394.